Supporting Information for

Highly Efficient Separation of Trivalent Minor Actinides by a Layered Metal Sulfide ($KInSn_2S_6$) from Acidic Radioactive Waste

Chengliang Xiao, [†,‡] Zohreh Hassanzadeh Fard, [‡] Debajit Sarma, [‡] Tze-Bin Song, [‡] Chao Xu,[*,§] and Mercouri G. Kanatzidis[*,‡]

[†] School for Radiological and Interdisciplinary Sciences (RAD-X) and Collaborative Innovation Center of Radiation Medicine of Jiangsu Higher Education Institutions, Soochow University, Suzhou 215123, China

[‡] Department of Chemistry, Northwestern University, 2145 Sheridan Road, Evanston, Illinois 60208, United States

[§] Collaborative Innovation Center of Advanced Nuclear Energy Technology, Institute of Nuclear and New Energy Technology, Tsinghua University, Beijing 100084, China

* xuchao@mail.tsinghua.edu.cn

* m-kanatzidis@northwestern.edu

Contents

EXPERIMENTAL SECTION

Materials.

Indium (4N, Strem Chemicals), tin (5N, American Elements), and sulfur (4N, Sigma-Aldrich) were used as received. K_2S_6 was prepared by reacting stoichiometric amounts of K and S elements in liquid ammonia. Radioactive ^{241}Am and ^{152}Eu were provided by China Institute of Atomic Energy and used for the batch sorption experiments. **Caution:** Extreme precautions must be taken in handling ^{241}Am and ^{152}Eu because of the radiation hazards. The experiments were conducted in a properly equipped laboratory following special regulatory requirements.

Synthesis of KMS-5.

KMS-5 was synthesized using two different methods: method (a) K_2CO_3 (0.022 mol , 3.109 g), Sn (0.06 mol, 7.122 g), In (0.03 mol, 3.444 g) and S (0.195 mol, 6.253 g) were combined and loaded in a 50 mL grinding jar under nitrogen atmosphere in a glove box. The mixture was ball-milled at 100 rpm for 1 min and at 250 rpm for 30 minutes. 3 g of the ball-milled mixture was placed in a 13 mm outer diameter (OD) carbon coated fused-silica tube under N_2 atmosphere. A rubber balloon was attached at the end of the reaction tube in order to accommodate the created pressure of the CO_2 evolution. The mixture was heated gradually to 200 °C where it was kept for 5 h before being successfully brought to 800 °C. It was kept at 800 °C for 8 h. Shiny yellow plate shape crystals were obtained by cooling at a rate of 40 °C/h to room temperature. The yield is about 78%.; method (b) A mixture of K_2S_6 (1 mmol, 0.270 g), S (6 mmol, 0.192 g), Sn (4 mmol, 0.475 g), and In (2 mmol, 0.229 g) was sealed under vacuum (10^{-4} Torr) in a 13 mm (OD) carbon coated fused-silica tube and heated (80 °C/h) to 800 °C. It was kept there for 24 h, followed by cooling to room temperature at 40 °C/h. The yield is about 80%. The empirical formula for the products obtained from two methods was $KInSn_2S_6$ based on EDS and ICP-OES analyses.

Ion Exchange Experiments.

Solutions of ^{241}Am and ^{152}Eu were prepared by mixing an aliquot of ^{241}Am and ^{152}Eu stock solution with HNO_3 solutions at a pre-adjusted pH. The concentration of ^{241}Am in

these solutions was determined to be around 2.4×10^{-8} M (or 5.6×10^{-6} g/L) by liquid scintillation counting on a LSC spectrometer (Quantulus 1220, Perkin Elmer). The V/m was fixed at 1000 mL/g (5 mg of sorbents in 5 mL of solution). After a certain time of mixing by magnetic stirring in 20 mL capped glass tube, solid-liquid phase separation was achieved by centrifugation. 100 μL of the clear aqueous phase was then sampled into a 20 mL of polyethylene vial (Perkin Elmer), into which 10 mL of commercially available cocktails OptiPhase Hisafe 3 (Perkin Elmer) was added. The solution was mixed by hand shaking and then the counts of ^{241}Am and ^{152}Eu were measured on the LSC spectrometer with previously established standard methods. The removal percentage (R) and K_d were calculated using the following equation, respectively.

$$K_d = \frac{V}{m}\frac{(C_i - C_f)}{C_f}$$

$$R = \frac{(C_i - C_f)}{C_i} \times 100\%$$

Where C_i and C_f represent the initial and final concentration (or counts) of Am or Eu in the aqueous solution, V is the volume (mL) of the solution and m is the mass of the sorbents.

The Langmuir and Freundlich models are used to fit the sorption isotherm of Eu^{3+} onto KMS-5. The Langmuir model assumes that the sorption of metal ions occurs on a homogenous surface by monolayer sorption and there is no interaction between adsorbed ions, with homogeneous binding sites and equivalent sorption energies. The linear equation of the Langmuir isotherm model is expressed as followed:

$$\frac{c_e}{q_e} = \frac{1}{q_m k_L} + \frac{c_e}{q_m}$$

where q_m is the maximum sorption capacity corresponding to complete monolayer coverage (mg/g) and k_L is a constant indirectly related to sorption capacity and energy of sorption (L/mg), which characterizes the affinity of the adsorbate with the adsorbent. The linearized plot was obtained when we plotted C_e/q_e against C_e and q_m and k_L could be calculated from the slope and intercept.

The Freundlich equation is an empirical equation based on sorption on a heterogeneous surface. The isotherm assumes that adsorbent surface sites have a spectrum of different binding energies. The linear equation can be expressed by:

$$\ln q_e = \ln k_F + \frac{1}{n} \ln c_e$$

where k_F and n are the Freundlich constants related to the sorption capacity and the sorption intensity, respectively. The linear plot was obtained by plotting $\ln q_e$ against $\ln c_e$, and the values of k_F and n were calculated from the slope and intercept of the straight line. Figures S6, S7, and Table S3 show the fitting results using the Langmuir and Freundlich equations.

To prepare the samples for characterization, we conducted the ion exchange reaction of KMS-5 (10 mg) in the aqueous solution containing 10 mmol of Eu^{3+} at pH 2. After 24 h, the samples were obtained after filtering and washing with water (three times) and acetone (three times).

Desorption Experiments

A sample from a previous pH dependence ion exchange experiment (pH 2) was centrifuged and the liquid phase was carefully removed from the tube, leaving the solid sorbents (5 mg) loaded with ^{241}Am in the glass tube. 5 mL of 1 M KCl solution was then added into the tube and mixed thoroughly with the sorbents by magnetic stirring for 120 min. After centrifugation, the liquid phase was sampled and measured by LSC spectrometer to obtain the concentration of ^{241}Am in the desorption solution. The desorption percentage (D) is defined as:

$$D = \frac{C_d}{C_s} \times 100\%$$

Where C_d is the concentration (counts/mL solution) of ^{241}Am in the final desorption solution and C_s represents the concentration (counts/mg sorbent) of ^{241}Am in the sorbents before desorption. C_s could be calculated from the results of previous adsorption experiment.

The details of the batch adsorption experiments are listed in **Table S1**.

Table S1. Batch experimental conditions.

Experiment	pH	Metal	Contacting time (min)	Temperature (°C)
Kinetics	2.0	^{241}Am (Trace amount) ^{152}Eu (Trace amount)	0, 2, 5, 10, 30, 60, 120, 240	25
pH dependence	0.5, 0.75, 1.0, 2.0, 3.0, 4.0, 5.0	^{241}Am (Trace amount) ^{152}Eu (Trace amount)	120	25
Selectivity	2.0	^{241}Am (Trace amount) ^{152}Eu (Trace amount) Na (Chloride): 10, 100, 1000, 23000 ppm Ca (Chloride): 10, 100, 1000 ppm Sr (Nitrate): 10, 1000 ppm Cs (Nitrate): 10, 1000 ppm Ni (Nitrate): 10, 1000 ppm	120	25
Capacity	2.0	^{152}Eu (Trace amount) Non-radioactive Eu: 5, 18, 45, 90, 180, 450, 675 ppm	120	25
Desorption	2.0	^{241}Am (Trace amount) ^{152}Eu (Trace amount) Desorption solution: 1 M KCl	120	25

Stability of KMS-5 at pH=2 measured by ICP

To quantitatively confirm the stability of KMS-5 in acidic solution, we have measured the concentration of indium using the inductively coupled plasma optical emission spectroscopy (ICP-OES, Spectro Arcos Sop, Germany) after immersing 10 mg of KMS-5 in 10 mL of aqueous solution at pH=2 as a function of contact time (Table S2). The maximum In concentration was 2.11 ppm, corresponding to the mass dissolved from KMS-5 was only 1.07%, which shows that KMS-5 is very stable under our experimental conditions, consistent with the results of PXRD very well.

Table S2. Concentration of indium dissolved in the aqueous after immersing KMS-5 in the aqueous solution at pH=2 as a function of contact time.

Contact time, min	In concentration, ppm	wt% of the KMS-5
10	0.24	0.12
30	0.09	0.04
70	2.01	1.02
150	2.11	1.07

Selective separation of ^{241}Am from the nuclear waste stream simulant

The nuclear waste stream simulant was prepared according to Table S3. After diluted to pH=2, ~5×10^{-3} ppm of ^{241}Am was added into the stream. Then 5 mg of KMS-5 was contacted with 5 mL of above stream under stirring for 120 min. After centrifugation, the liquid phase was sampled and measured by LSC spectrometer to obtain the concentration of ^{241}Am in the desorption solution. It is found that nearly 97.7% of ^{241}Am was removed from the nuclear stream simulant by KMS-5.

Table S3. Composition of nuclear waste stream simulants

Metal	Concentration, g/L	Metal	Concentration, g/L
Ba	0.379	Pd	0.303
Cd	0.037	Pr	0.224
Ce	0.468	Rb	0.069
Cr	0.062	Rh	0.076
Cs	0.449	Ru	0.451
Eu	0.027	Sm	0.148
Fe	0.237	Sn	0.017
Gd	0.038	Sr	0.142
La	0.24	Te	0.096
Mo	0.674	Tc	0.141
Na	1.136	Y	0.089
Nd	0.801	Zr	0.716
Ni	0.046	HNO_3	3 M

Characterizations.

SEM-EDS graphs were obtained by a Hitachi S3400N-II scanning electron microscope equipped with an ESED II detector. The powder X-ray Diffraction (PXRD) patterns were obtained using a Rigaku Miniflex powder X-ray diffractometer with Ni-filtered Cu Kα radiation operating at 30 kV and 15 mA. Single crystal data were

collected on a STOE IPDS II diffractometer using Mo Kα radiation at room temperature. The generator was operated at 50 kV and 40 mA. The data were collected with a scan width of 1° keeping the crystal to detector distance fixed at 8.0 cm. The structure was solved using direct methods and refined by the SHELXTL program package using a full-matrix least squares refinement against the square of structure factors. Final structure refinement included atomic positions and anisotropic thermal parameters for all Sn/In and S atoms. The UV-vis/NIR diffuse reflectance spectra were measured using a Shimadzu UV03010 PC spectrophotometer. $BaSO_4$ powder was used as a reference and base material. X-ray photoelectron spectroscopy (XPS) of KMS-5 and KMS-5-Eu were conducted on a Thermo Scientific ESCALAB 250 Xi spectrometer equipped with a monochromatic Al Kα X-ray source (1486.6 eV) operating at 300 W. Samples were analyzed under vacuum ($P < 10^{-8}$ mbar) with a pass energy of 150 eV (survey scans) or 25 eV (high-resolution scans). All peaks were calibrated with C 1s peak binding energy at 284.7 eV for adventitious carbon. The experimental peaks were fitted with Avantage software.

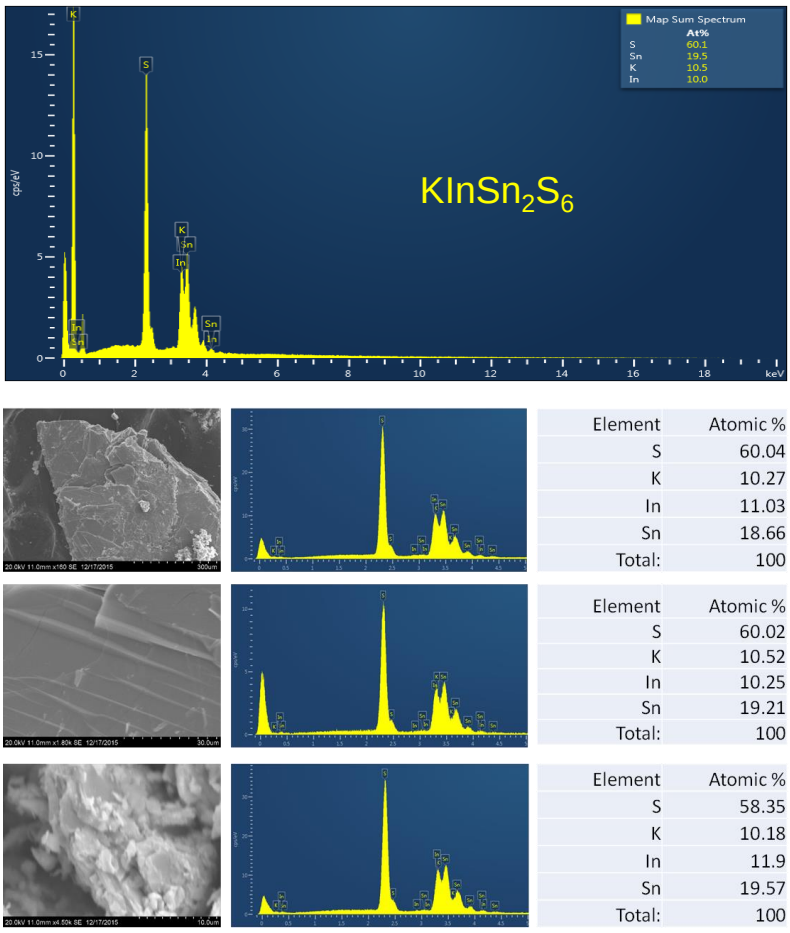

Figure S1. EDS result of KMS-5, which confirms that the formula is $KInSn_2S_6$.

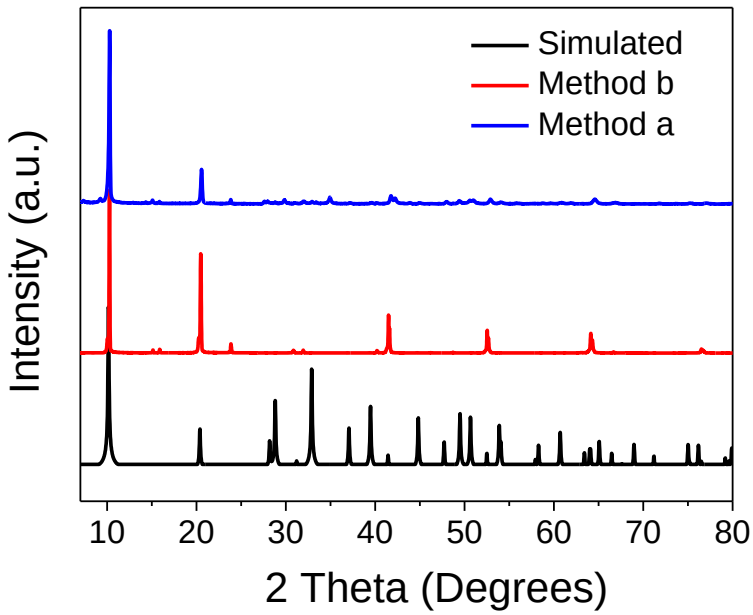

Figure S2. PXRD patterns of calculated and experimental KMS-5.

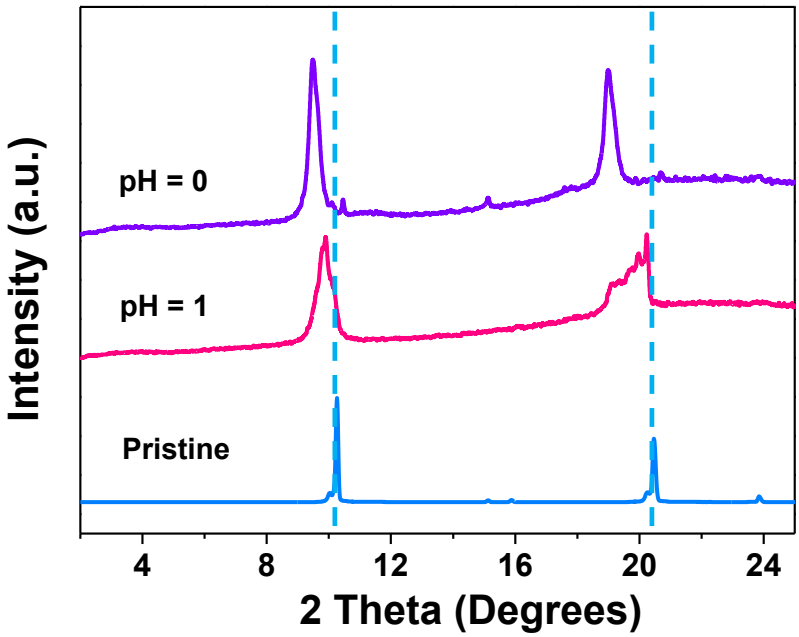

Figure S3. Enlarged PXRD patterns (2-25°) of KMS-5 before and after immersed in acidic solution at pH 0 and 1.

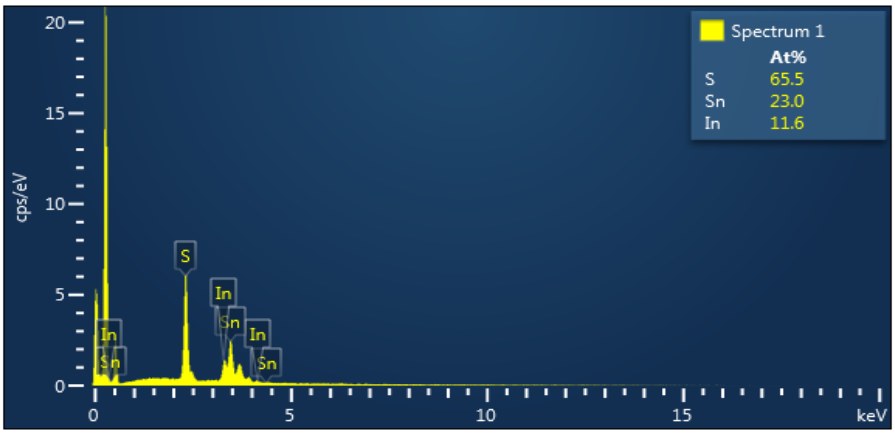

Figure S4. EDS result of KMS-5 after immersed in acidic solution at pH 0.

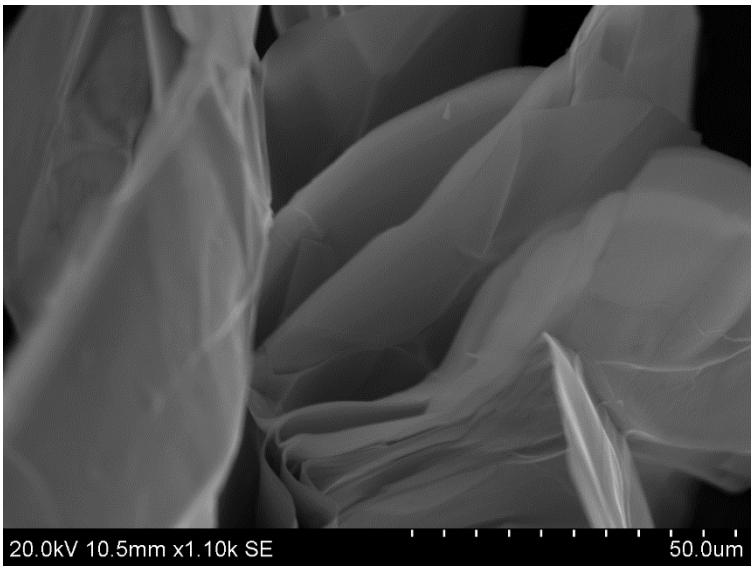

Figure S5. SEM image of KMS-5 after immersed in acidic solution at pH 0.

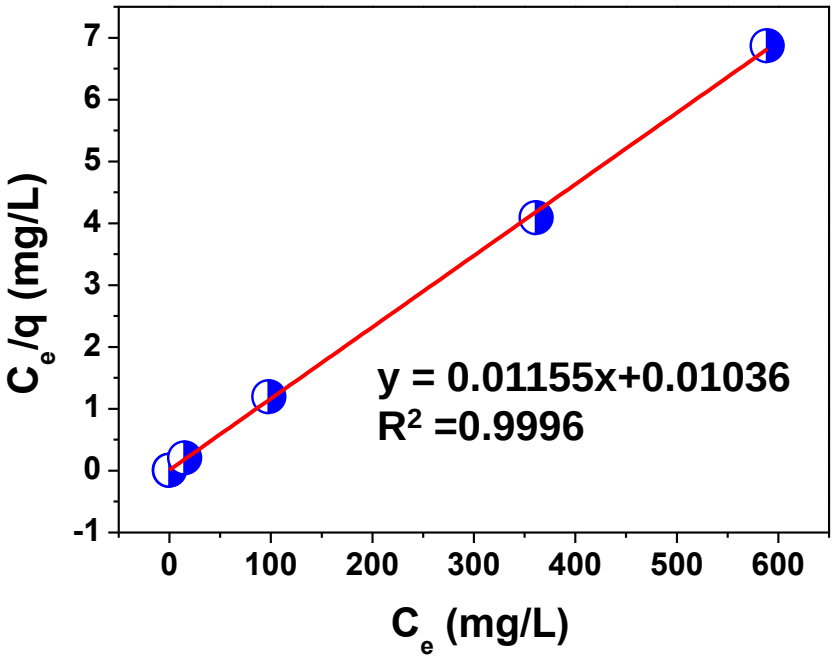

Figure S6. Fitting curve for sorption isotherm of Eu^{3+} by KMS-5 using Langmuir model.

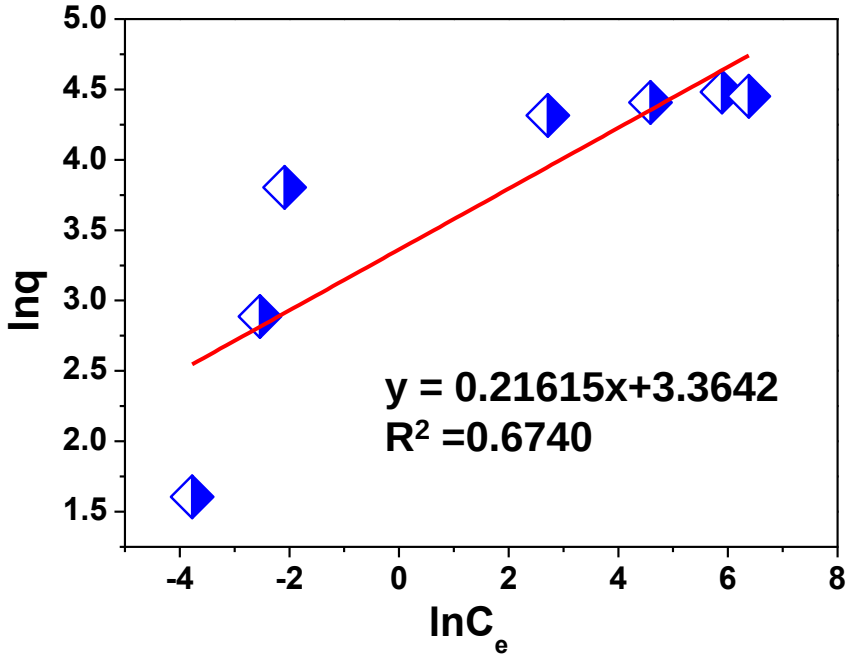

Figure S7. Fitting curve for sorption isotherm of Eu^{3+} by KMS-5 using Freundlich model.

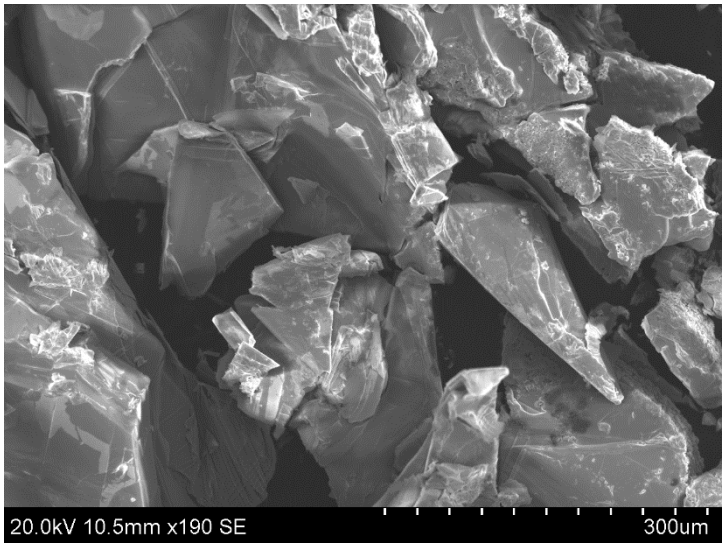

Figure S8. SEM image of KMS-5 after exchanged with Eu^{3+}.

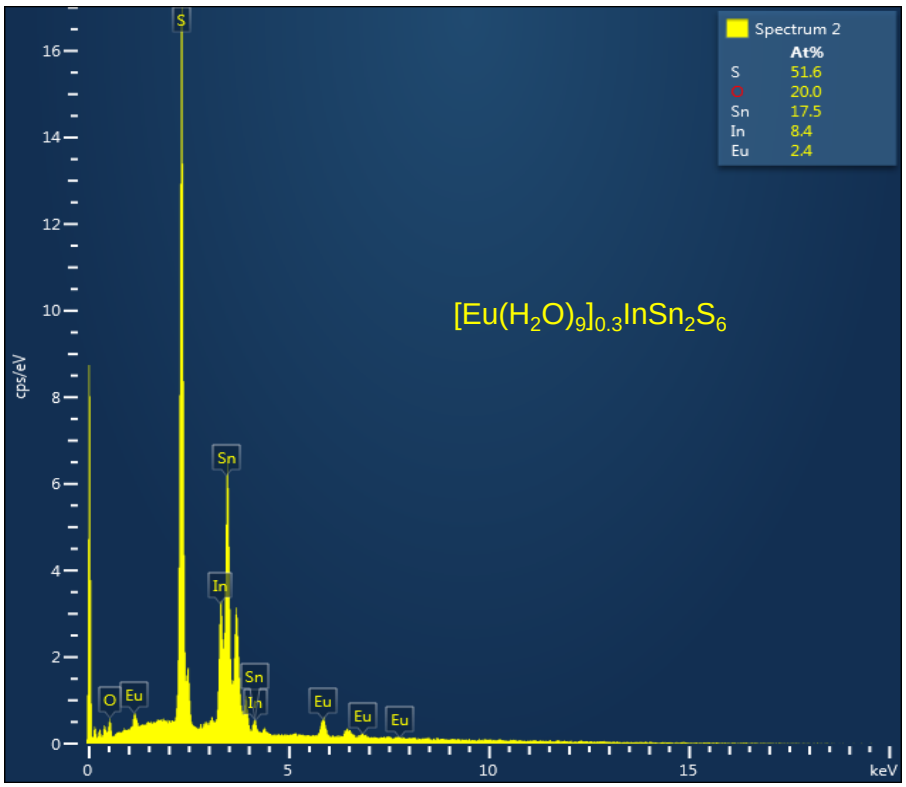

Figure S9. EDS of Eu^{3+}-exchanged KMS-5.

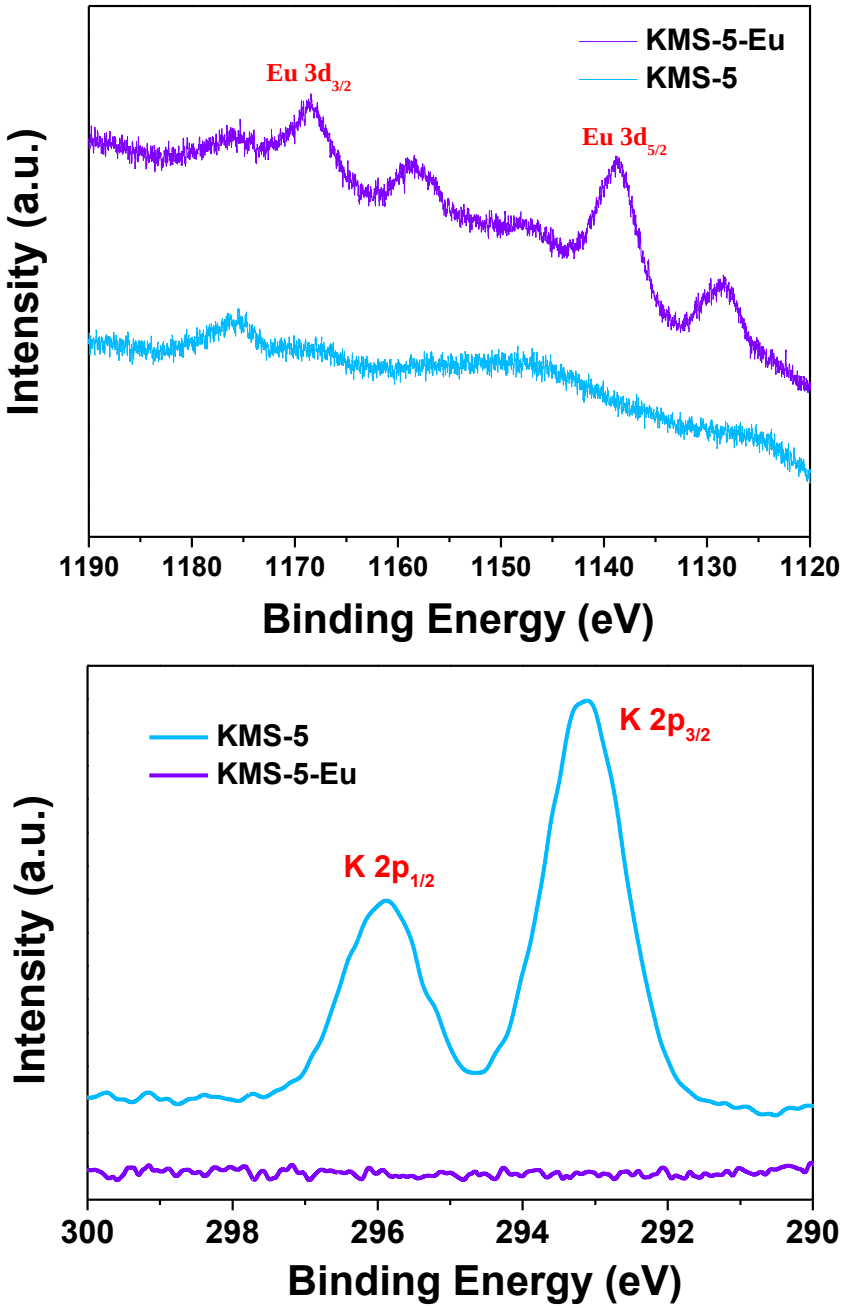

Figure S10. Narrow scan XPS spectra of Eu 3d and K 2p of KMS-5 and KMS-5-Eu.

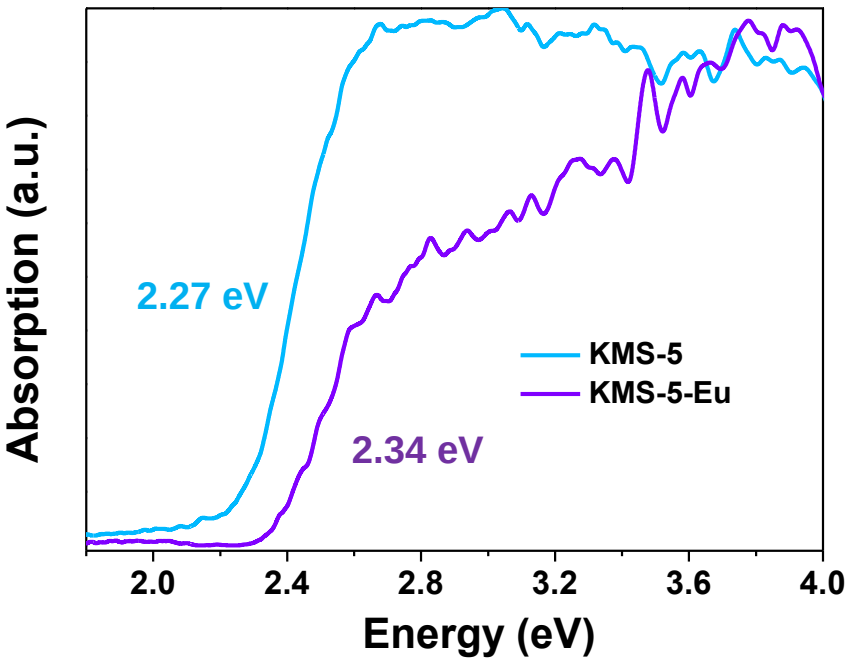

Figure S11. Solid-state optical absorption spectra of the KMS-5 and KMS-5-Eu samples.

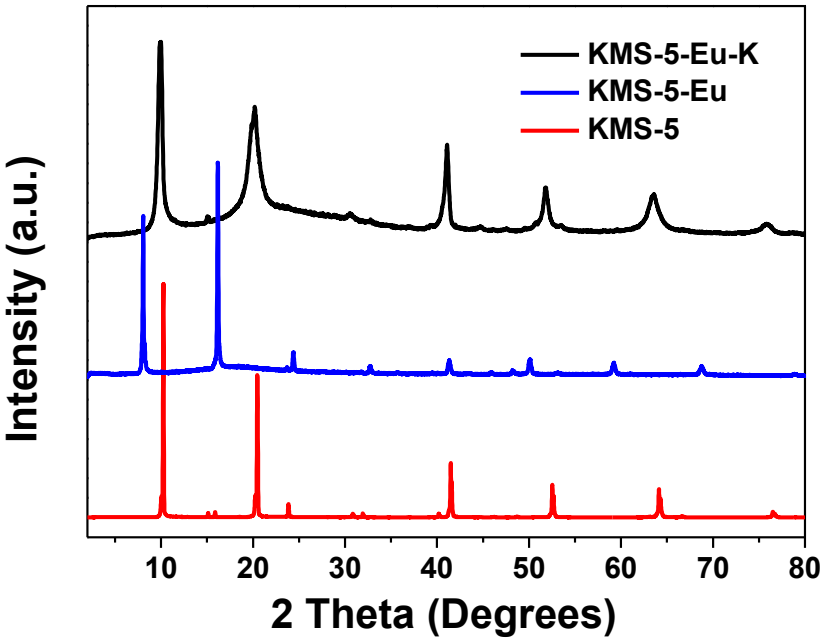

Figure S12. PXRD patterns of KMS-5-Eu samples before and after elution with 1M KCl.

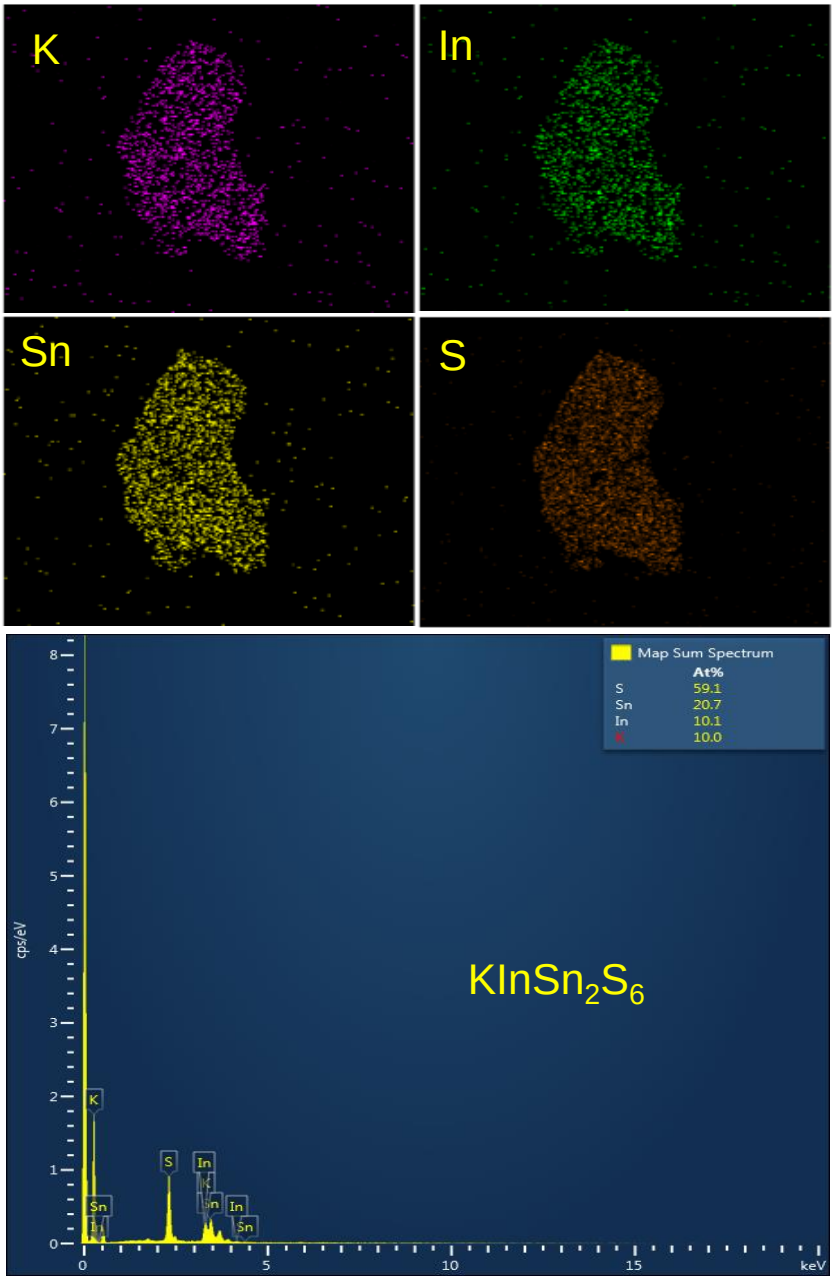

Figure S13. SEM-EDS data of KMS-5-Eu samples after elution with 1M KCl.

Table S4. Crystal data and structure refinement for $KInSn_2S_6$ (KMS-5) at 100(2) K.

Empirical formula	$KInSn_2S_6$
CCDC no.	1576878
Formula weight	583.66
Temperature	100(2) K
Wavelength	0.71073 Å
Crystal system	trigonal
Space group	R-3m
Unit cell dimensions	a = 3.68030(10) Å, α = 90° b = 3.68030(10) Å, β = 90° c = 26.1276(16) Å, γ = 120°
Volume	306.48(3) $Å^3$
Z	1
Density (calculated)	3.162 g/cm^3
Absorption coefficient	7.208 mm^{-1}
F(000)	264
Crystal size	0.280 × 0.280 × 0.120 mm^3
θ range for data collection	4.681 to 27.864°
Index ranges	$-4 \le h \le 4$, $-4 \le k \le 4$, $-33 \le l \le 33$
Reflections collected	2654
Independent reflections	124 [R_{int} = 0.0383]
Completeness to θ = 25.242°	99%
Refinement method	Full-matrix least-squares on F^2
Data / restraints / parameters	124 / 12 / 13
Goodness-of-fit	1.091
Final R indices [I > 2σ(I)]	R_{obs} = 0.0308, wR_{obs} = 0.1090
R indices [all data]	R_{all} = 0.0308, wR_{all} = 0.1090
Largest diff. peak and hole	3.000 and -0.510 e·$Å^{-3}$

$R = \Sigma||F_o|-|F_c||/\Sigma|F_o|$, $wR = \{\Sigma[w(|F_o|^2-|F_c|^2)^2] / \Sigma[w(|F_o|^4)]\}^{1/2}$ and $w=1/[\sigma^2(F_o^2)+(0.1000P)^2+0.3333P]$ where $P=(F_o^2+2F_c^2)/3$

Table S5. Atomic coordinates (×104) and equivalent isotropic displacement parameters (Å^2×103) for KMS-5. U(eq) is defined as one third of the trace of the orthogonalized U^{ij} tensor.

	x	y	z	U(eq)
In(1)	0	0	0	7(1)
Sn(1)	0	0	0	7(1)
S(1)	3333	6667	554(1)	9(1)
K(1)	-1667	6667	1667	20(7)
K(2)	0	0	1660(15)	27(7)

Table S6. Anisotropic displacement parameters (Å^2×10^3) for KMS-5. The anisotropic displacement factor exponent takes the form: $-2p^2[\, h^2a^{*2}U^{11} + \ldots \quad + 2h\,k\,a^*\,b^*U^{12}\,]$

	U^{11}	U^{22}	U^{33}	U^{23}	U^{13}	U^{12}
In(1)	2(1)	2(1)	17(1)	0	0	1(1)
Sn(1)	2(1)	2(1)	17(1)	0	0	1(1)
S(1)	6(1)	6(1)	13(1)	0	0	3(1)
K(1)	25(10)	32(10)	6(8)	-3(8)	-1(4)	16(5)
K(2)	33(8)	33(8)	14(9)	0	0	17(4)

Table S7. Ion exchange properties of ^{152}Eu and ^{241}Am by KMS-5 as a function of pH.

radionuclides	pH	V/m	initial	final	%removal	K_d, mL/g
^{152}Eu	0.5	1000	3864	1936	50.1	9.47×10^2
	1	1000	3496	166	95.3	2.01×10^4
	2.02	1000	4479	77	98.3	5.72×10^4
	3.02	1000	4000	488	87.8	7.2×10^3
	4	1000	3749	350	90.7	9.71×10^3
	5.03	1000	3420	685	80.0	3.99×10^3
^{241}Am	0.5	1000	4052	2087	51.5	1.06×10^3
	1	1000	3956	137	96.5	2.79×10^4
	2.02	1000	4264	71	98.3	5.91×10^4
	3.02	1000	3967	640	83.9	5.20×10^3
	4	1000	3664	399	89.1	8.18×10^3
	5.03	1000	2949	672	77.2	3.39×10^3

Table S8. Comparison of the largest distribution coefficients (K_d, mL/g) of ^{241}Am uptake by different sorbents.

Samples	K_d, pH = 1	K_d, pH = 2	Ref.
Nano-cerium vanadate	~20	2.5×10^2	[1]
P-BTP	-	60	[2]
SBA-POH	$\sim1.4\times10^2$	$\sim2.2\times10^2$	[3]
MCM-POH	~40	~60	[3]
BPMO-POH	~90	$\sim1.2\times10^2$	[3]
BTPhen/SiO_2	4.88×10^3	-	[4]
Monosodium titanate	~60	-	[5]
BPP-7	-	1.58×10^2	[6]
Tin phosphonate	1.0×10^3	2.9×10^4	[7]
Graphene oxide	$<10^3$	1.94×10^4	[8]
KMS-5	2.79×10^4	5.91×10^4	This work

Table S9. Fitting results from the Langmuir and Freundlich isotherm models.

Samples	Langmuir			Freundlich		
	q_m (mg g^{-1})	b (L mg^{-1})	R^2	k_F(L^n/mol^{n-1} g)	n	R^2
KMS-5	86.58	1.11	0.9996	28.91	4.62	0.6740

Table S10. Comparison of sorption capacity of Eu^{3+} by different materials.

Materials	pH	Temperature, K	Capacity, mg/g	Ref.
TiO_2	4.5	293	1.51	[9]
ZSM-5 zeolite	3.62	298	2.42	[10]
Al_2O_3/EG	4.0	293	4.74	[11]
Fe_3O_4@HA MNPs	5.0	293	10.56	[12]
sepiolite	6.0	303	22.85	[13]
activated carbon	5.0	298	46.5	[14]
titanium phosphate @graphene oxide	5.5	298	64.33	[15]
FJSM-SnS	4.0	333	139.82	[16]
graphene oxide	6.0	298	175.44	[17]
KMS-5	2.0	298	86.58	this work

References

(1) Banerjee, C.; Dudwadkar, N.; Tripathi, S. C.; Gandhi, P. M.; Grover, V.; Kaushik, C. P.; Tyagi, A. K., *J Hazard. Mater.* **2014,** *280*, 63-70.

(2) Veliscek-Carolan, J.; Jolliffe, K. A.; Hanley, T. L., *Chem. Commun.* **2015,** *51*, 11433-11436.

(3) Zhang, W.; He, X.; Ye, G.; Yi, R.; Chen, J. *Environ. Sci. Technol.* **2014,** *48*, 6874-6881.

(4) Afsar, A.; Distler, P.; Harwood, L. M.; John, J.; Westwood, J., *Chem. Commun.* **2017,** *53*, 4010-4013.

(5) Shehee, T. C.; Elvington, M. C.; Rudisill, T. S.; Hobbs, D. T. *Solv. Extr. Ion Exch.* **2012,** *30*, 669-682.

(6) Demir, S.; Brune, N. K.; Van Humbeck, J. F.; Mason, J. A.; Plakhova, T. V.; Wang, S.; Tian, G.; Minasian, S. G.; Tyliszczak, T.; Yaita, T.; Kobayashi, T.; Kalmykov, S. N.; Shiwaku, H.; Shuh, D. K.; Long, J. R. *ACS Cent. Sci.* **2016,** *2*, 253-65.

(7) Silbernagel, R.; Shehee, T. C.; Martin, C. H.; Hobbs, D. T.; Clearfield, A. *Chem. Mater.* **2016,** *28*, 2254-2259.

(8) Romanchuk, A. Y.; Slesarev, A. S.; Kalmykov, S. N.; Kosynkin, D. V.; Tour, J. M. *Phys. Chem. Chem. Phys.* **2013,** *15*, 2321-2327.

(9) Tan, X.; Fang, M.; Li, J.; Lu, Y.; Wang, X. *J. Hazard. Mater.* **2009**, *168*, 458-465.

(10) Shao, D.; Fan, Q.; Li, J.; Niu, Z.; Wu, W.; Chen, Y.; Wang, X. *Micropor. Mesopor. Mater.* **2009**, *123*, 1-9.

(11) Sun, Y.; Chen, C.; Tan, X.; Shao, D.; Li, J.; Zhao, G.; Yang, S.; Wang, Q.; Wang, X. *Dalton Trans.* **2012**, *41*, 13388-13394.

(12) Yang, S.; Zong, P.; Ren, X.; Wang, Q.; Wang, X., *ACS Appl. Mater. Interfaces* **2012**, *4*, 6890-6899.

(13) Sun, Y.; Li, J.; Wang, X., *Geochim. Cosmochim. Acta* **2014**, *140*, 621-643.

(14) Gad, H. M. H.; Awwad, N. S. *Sep. Sci. Technol.* **2007**, *42*, 3657-3680.

(15) Li, C.; Huang, Y.; Lin, Z. *J. Mater. Chem. A* **2014**, *2*, 14979-14985.

(16) Qi, X. H.; Du, K. Z.; Feng, M. L.; Gao, Y. J.; Huang, X. Y.; Kanatzidis, M. G. *J. Am. Chem. Soc.* **2017,** *139*, 4314-4317.

(17) Sun, Y.; Wang, Q.; Chen, C.; Tan, X.; Wang, X., *Environ. Sci. Technol.* **2012**, *46*, 6020-6027.